Int J Earth Sci (Geol Rundsch) (2002) 91:615–628
DOI 10.1007/s00531-001-0245-8

ORIGINAL PAPER

T.R. Walter · H.-U. Schmincke

Rifting, recurrent landsliding and Miocene structural reorganization on NW-Tenerife (Canary Islands)

Received: 28 February 2001 / Accepted: 19 November 2001 / Published online: 1 June 2002

Abstract We studied mechanisms of structural destabilization of ocean island flanks by considering the linkage between volcano construction and volcano destruction, exemplified by the composite Teno shield volcano on Tenerife (Canary Islands). During growth, Tenerife episodically experienced giant landslides, genetically associated with rifting and preferentially located between two arms of a three-armed rift system. The deeply eroded late Miocene Teno massif allows insights into the rifting processes, the failure mechanisms and related structures. The semicircular geometry of palaeo-scarps and fracture systems, breccia deposits and the local dike swarm reconfigurations delineate two clear landslide scarp regions. Following an earlier collapse of the older Los Gigantes Formation to the north, the rocks around the scarp became fractured and intruded by dikes. Substantial lava infill and enduring dike emplacement increased the load on the weak scarp and forced the flank to creep again, finally resulting in the collapse of the younger Carrizales Formation. Once more, the changing stress field caused deformation of the nearby rocks, a fracture belt formed around the scarp and dikes intruded into new (concentric) directions. The outline, size and direction of the second failed flank of Teno very much resembles the first collapse. We suggest structural clues concerning mechanisms of recurrent volcano flank failure, verifying the concept that volcano flanks that have failed are prone to collapse again with similar dimensions.

Keywords Canary Islands · Dike reconfiguration · Flank instability · Recurrent sector collapse · Volcano spreading

T.R. Walter (✉) · H.-U. Schmincke
GEOMAR, Dept. of Volcanology and Petrology,
Wischhofstr. 1-3, 24148 Kiel, Germany
e-mail: twalter@geomar.de

T.R. Walter
Graduate School 'Dynamics of Global Cycles'
of the Christian-Albrechts-University Kiel at GEOMAR,
Wischhofstr. 1-3, 24148 Kiel, Germany

Introduction

Volcanic islands are structurally unstable and thus susceptible to seaward-directed mass wasting. The lateral collapse of huge sectors of a volcano can be highly destructive, and be manifested in debris avalanches, volcanic explosions and tsunamis. Despite the hazard-potential of volcanoes, the structural mechanisms relating to the size, frequency and direction of giant landslides are poorly understood.

Volcanoes are predisposed to spread outwards because of their topographic load and their intrusive complexes that tend to decouple the stress field (Fiske and Jackson 1972; Borgia 1994). Intrusions frequently form rift zones, defined by parallel swarms of (feeder) dikes and topographic ridges of aligned vents, which are prominent structural features of ocean-island volcanoes (Stillman 1987; Walker 1992). The lateral collapse of volcanic edifices is commonly structurally linked to those rift zones (Siebert 1984).

To reconstruct the volcano-tectonic palaeo-stress field controlling the emplacement of a dike-swarm, detailed studies of dike arrangements are required. The direction of a propagating dike typically tends to be perpendicular to the minimum principal compressive stress, allowing us to study the palaeo-stress relations within a volcanic edifice at the time of dike emplacement (Anderson 1937). Structural field data have been used in the past to study the tectonic evolution of the Canary Islands (Schmincke 1968; Féraud et al. 1985; Stillman 1987; Barrera et al. 1989; Carracedo 1994, 1996; Martí et al. 1997; Marinoni and Gudmundsson 2000). Some rift zones formed during the entire evolution of a volcanic island extending over 50 km from a nucleus (Fig. 1). These rift zones are initiated most commonly during the shield-building stage of an island and –once established– imply the locations of unstable volcano sectors. On La Palma, an unstable flank is sited normal to a major north–south rift zone (Day et al. 1999). Failures of El Hierro and Tenerife often bisect the angles formed by two structural axes of persistent diking, whereas mag-

matic activity concentrated along three structural axes to form morphological ridges and triangular elongated edifices (Navarro and Farrujia 1989; Carracedo 1994, 1996). The collapse of huge volcanic sectors into the sea has produced additional serrate shorelines (Carracedo 1994; Krastel et al. 2001).

Here, we report the results of detailed field studies that focus on the late Miocene basaltic shield of Teno (northwestern Tenerife), with an attempt to infer the palaeo-stress that constrained the brittle deformation and several dike arrangements. Deep erosion of the Teno volcano has revealed a relationship between dike emplacement and major sector collapses. The data analysis of ~800 measured dikes and fractures allows us to estimate the local tectonic evolution, which was significantly influenced by near-surface effects. We describe the substantial intrusive activity focused on the Teno rift zones, and the modification of dike traces linked to recurrent collapses of volcano sectors.

The aim of this study is to better understand the mechanisms of volcano deformation and flank destabilization, sector collapse and the structural aspects that act together. This study may help to focus studies on volcanic edifices that are in-between two sector collapse events.

Volcano-tectonic evolution of Tenerife

Tenerife is the highest island of the Canaries and is centrally located in the Archipelago. The oldest subaerial rocks of Tenerife are those of three separate basaltic shield volcanoes on the corners of the island, composed mainly of alkali basalts, basanite, ankaramite and minor phonolite and trachyte, emplaced between 12 and 3.3 Ma (Ancochea et al. 1990; Thirlwall et al. 2000). These Miocene series expose at the eroded volcanic massifs Roque del Conde, Anaga and Teno (Fig. 1). Mainly basaltic and phonolitic eruptions formed the huge Las Cañadas edifice, starting at around 3.5 Ma ago (Ancochea et al. 1990; Martí et al. 1997). The volcano-tectonic evolution of this pivotal edifice was dominated by rifting, which was concentrated in three rift arms that diverge from the Las Cañadas center to the northeast, to the northwest and to the south (Ancochea et al. 1990; Carracedo 1994). The internal structural design of Tenerife was earlier inferred from gravity data, also showing density zones in triaxial geometry (McFarlane and Ridley 1968). However, the existence of an active southern rift zone is questioned (cf. Martí et al. 1996). The main structural axis of Tenerife during its Pliocene and Pleistocene evolution is the southwest–northeast ridge (Cordillera Dorsal) between the Las Cañadas Volcano and the Anaga Massif, forming basaltic lavas and scoria cones. The major rifts of Tenerife overlap with shorter, secondary structural axes (Fig. 1), probably defining separate volcanic centers (Navarro and Farrujia 1989; Navarro and Coello 1989), but flank collapses destroyed large parts of such centers to form the scarps, e.g. of Güimar and La Orotava. At least six north-directed flank

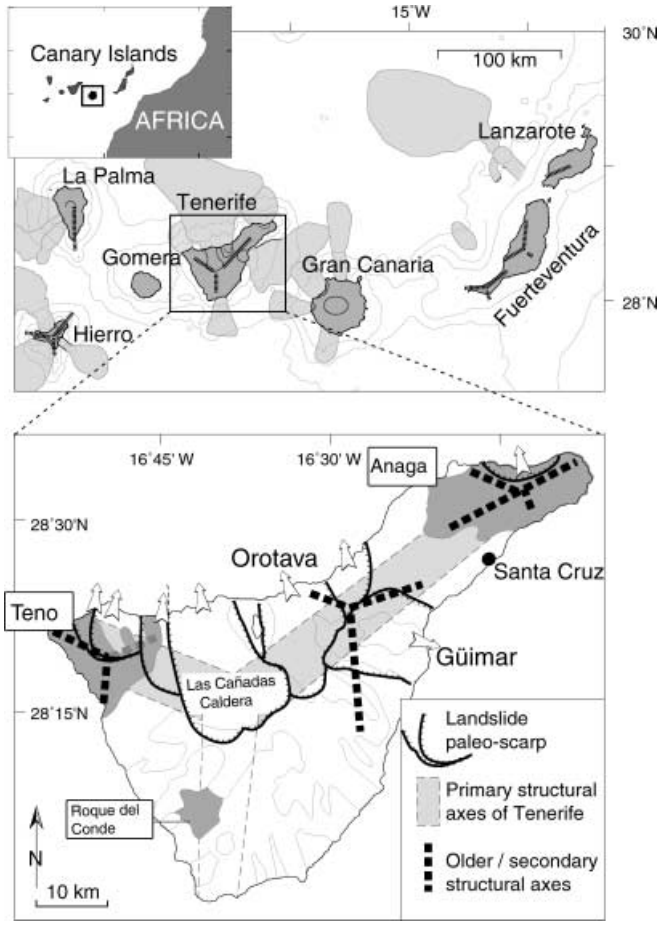

Fig. 1 Location of the Canary Islands and structural axes of rift zones (after Féraud et al. 1985; Carracedo 1996). Areal distribution of submarine debris avalanche, debris flow and slump deposits after Krastel et al. (2001). *Enlarged inset* showing Tenerife with inferred structural axes and sites of lateral failures (after Navarro and Farrujia 1989; Carracedo 1994; authors' unpublished results). *Shaded areas* represent the Miocene shield volcanoes of Anaga, Roque del Conde and Teno

collapses have been documented (Ancochea et al. 1990; Cantagrel et al. 1999; Hürlimann et al. 1999; Ablay and Hürlimann 2000; Watts and Masson 2001) generating submarine landslide deposits that cover several thousands of square kilometers north of Tenerife (Teide Group 1997; Watts and Masson 2001). The most recent giant landslide formed when the upper part of the Las Cañadas edifice failed ~0.18 Ma ago north of the present scarp of the 'Las Cañadas Caldera' (Navarro and Coello 1989; Ancochea et al. 1990; Watts and Masson 2001), interpreted by some authors as mainly caused by vertical caldera collapse (Martí et al. 1997). A giant explosion formed when the active magmatic/hydrothermal system of the Las Cañadas volcano was decapitated, leaving an extremely widespread blast deposit on Tenerife (Schmincke et al. 1999). The morphological Las Cañadas depression was subsequently filled by the Teide-Pico Viejo complex that towers 3,718 m high.

The episodes of volcano growth were periodically interrupted by unstable flanks that failed seawards – a pro-

cess that had already affected late Miocene palaeo-Tenerife. Numerous dike swarms and fracture sets form structural unconformities in the Teno complex, which preserve a complex record of volcano deformation. A palaeo-stress reconstruction of the Miocene massifs, Teno and Anaga, based on dikes and fault planes, revealed extensional tectonics without traces of major compression, inferring three major tectonic episodes: (1) a pre-intrusive dip-slip fault extension trending NE–SW; (2) an extension trending WNW–ESE with oblique to strike-slip faulting; and (3) a strong late/post-intrusive extension trending NE–SW (Marinoni and Gudmundsson 2000). Local influences on these deformational episodes related to sector collapses were, however, not considered. The origin of the reorientation of the stress field principal axes was not established; it may include island-size gravitational effects because of island growth.

Table 1 Structural evolution of Teno. The three major stages of Teno are unconformity bounded. Note the changing quantity of dikes before and after a sector collapse event. The intrusive activity along the rift zones decreased, whereas concentric dike directions sequentially increased. The maximum extensional strain e (%) measured by dikes was computed for 100-m profile units

Time Ma	Construction	Destruction	Dike swarms	Max. e [%] of dikes
	El Palmar Formation		Concentric	8
			Radial	3
			Mazca Rift	3
6	Unconformity-2	Carrizales Collapse	Teno Bajo Rift	7
	Carrizales Formation	Los Gigantes Collapse	Concentric	4
	Unconformity-1		Radial	1
			Mazca Rift	?
	Los Gigantes Formation		Teno Bajo Rift	19
7			Mazca Rift	28
			Teno Bajo Rift	10
			NE-SW?	

The structure of Teno

The Teno massif in NW-Tenerife is strongly eroded, with deep seaward-trending canyons (barrancos). The maximum elevation of ridges more than 1,300 m asl alternates with 500-m-deep barrancos, frequently with >200-m-high vertical cliffs that allow detailed structural analyses.

Neglecting minor post-Miocene volcanic and sedimentary deposits, the Teno composite shield is largely underlain by aa and pahoehoe basalt lavas erupted between 7.4 and 5.0 Ma, belonging to the ‘Old Basaltic Series’ of Tenerife (Ancochea et al. 1990). New geochronological data indicate a very rapid history of Teno in Messinian age, forming the vast bulk of the massif in a time interval between 6.4 and 6.0 Ma (Thirlwall et al. 2000; Bogaard unpublished Ar-Ar data).

The Teno composite shield (see Table 1) is here reconstructed using unconformity-bounded stratigraphic units. An angular unconformity defines two subseries for Teno, termed ‘lower sequence’ and ‘upper sequence’ by Ancochea et al. (1990). We identified two irregular unconformities marked by individual polymict debris deposits, separating three major evolutionary stages of Teno. We here name the three series based on well-exposed localities Los Gigantes Formation (LGF), Carrizales Formation (CF) and El Palmar Formation (EPF).

The Los Gigantes Formation largely forms the deeply eroded cliff of Los Gigantes south of Teno Bajo in southwestern Teno (Fig. 2) by a sequence of predominantly basaltic, <1-m-thick lava flows, which are frequently clastic and dip up to 40° to the western shoreline. Reddish scoria deposits and local unconformities are common. Phonolites occur in the top of the formation such as the up to 80-m-thick glassy phonolitic agglutinate with discontinuous basaltic spatter lenses, at 700 m asl southeast of the village of Mazca. Most of the Los Gigantes Formation is formed by steeply inclined pahoehoe flows and is covered unconformably by sub-horizontal lavas of the Carrizales Formation. The unconformity separating these two formations represents the trace of a ~6-Ma-old landslide, and is marked by the presence of a polymict breccia (Cantagrel et al. 1999). The lava flows of the Carrizales Formation are mostly 1–2 m thick and are characteristically rich in fresh olivine and pyroxene, forming picritic lava flows (e.g. near the village of Los Carrizales). In addition, the Carrizales Formation clearly differs from the underlying lavas in showing fewer dikes and scoria cones. A second angular unconformity separates the Carrizales Formation from the overlying El Palmar Formation (Fig. 3). The El Palmar Formation consists of generally horizontal basaltic and minor phonolitic and trachytic flows. The eroded formation is still >700 m thick with an age at its top of ~5.0 Ma (Ancochea et al. 1990).

Both unconformities are overlain by polymict debrites defining abrupt scarps, which enclose horseshoe-shaped areas similar in size and open towards the NNE. Moreover, the dip and strike of the unconformities is generally very similar. We analyzed numerous fractures that characterize the volcano deformation and the linked flank instability. Dikes emplaced following flank failure intruded along new directions. Named by the formation that failed, the first Teno sector collapse is called the Los Gigantes collapse; the second collapse is the Carrizales collapse. The arrangements of dikes and fractures are tentatively grouped into pre- and post-collapse swarms (Table 1). Analyzing the fractures, we distinguish between faults with a measurable displacement >5 cm, and fractures with smaller displacements. Most fractures in Teno, however, are joint sets without obvious mismatch. The structural arrangement of dikes and displacing fractures was studied in detail along nine profiles (Fig. 2d) and statistically analyzed in stereographic projections (Fig. 4).

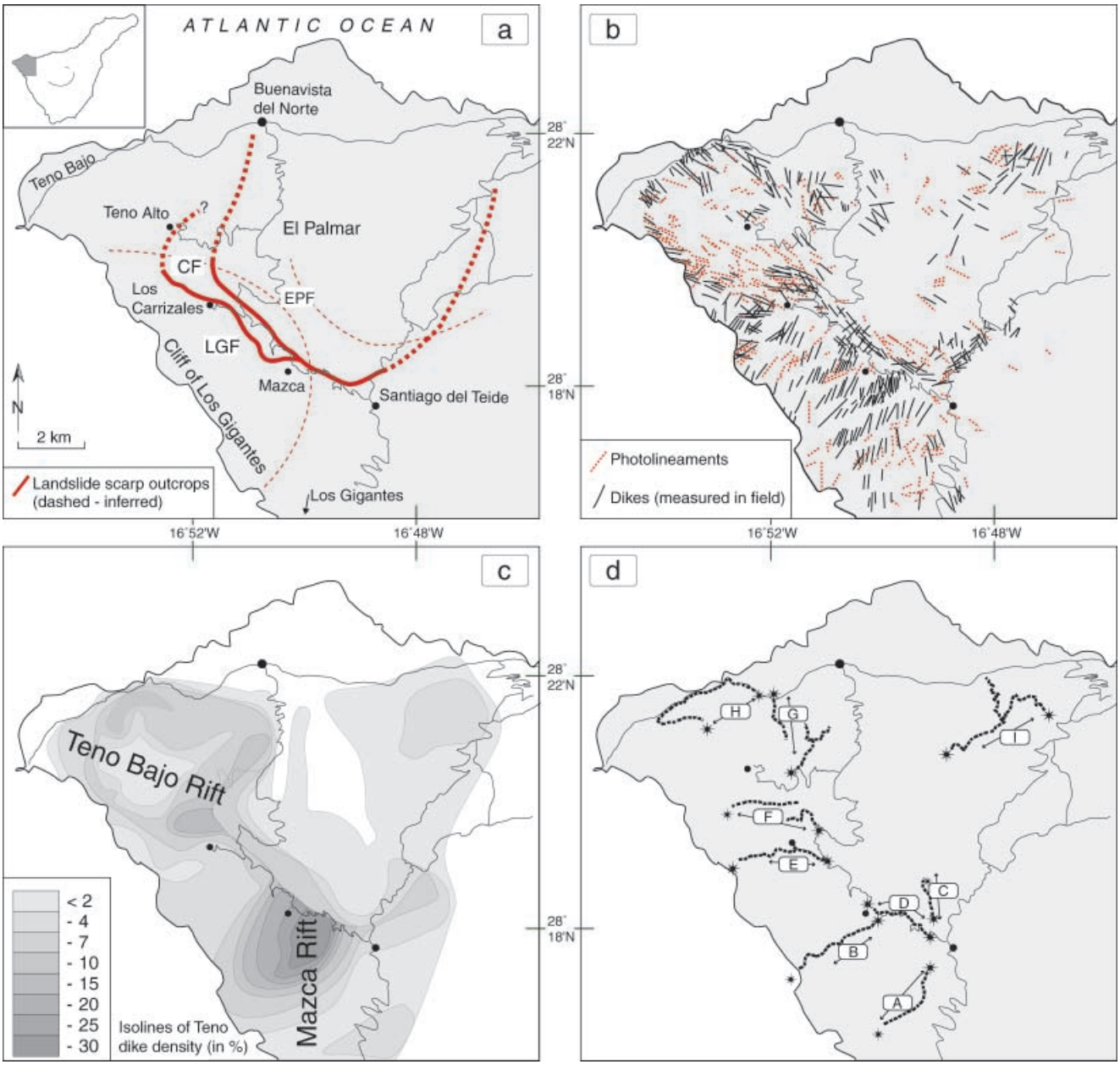

Fig. 2 Maps of Teno with **a** outline of the palaeo-scarps, **b** summarizing dike orientations as measured in the field (*solid lines*) and studied in aerial photographs (*dashed lines*), **c** isolines of dike density, calculated for a 0.5-km grid, **d** locations of nine profiles (*A–I*) studied in detail

Los Gigantes collapse

The western unconformity is marked by flat inclined infill, as well as well-mixed, heterolithological debrites (debris flows deposits) and local interbedded scoria deposits, inclined around 30° to the north-northeast (e.g. 1 km south of Los Carrizales). The lower part of scarp infill is noteworthy; lava flows being very rich in phenocrysts up to 3 cm in diameter and up to 50% of the rocks volume. From base to about 80 m of infill thickness, the petrography gradually changes from plagioclase-rich, towards olivine- and clinopyroxene-rich, picritic and occasionally dunitic lava flows. Crystal segregation, the absence of cooling units and load casts between the individual lava flows indicate low viscosity and rapid eruption and emplacement of this sequence following Carrizales collapse, possibly accelerated due to a decompressed magmatic system. The subhorizontal dip of the sequence suggests the eruptive center to have been located inside the depression, refilling it from inside.

The debrite formed from the amphitheater downwards, accumulating up to 4 to 8 m thickness and dipping towards the valley of El Palmar in the north-northeast. The outline of this polymict debrite defines part of

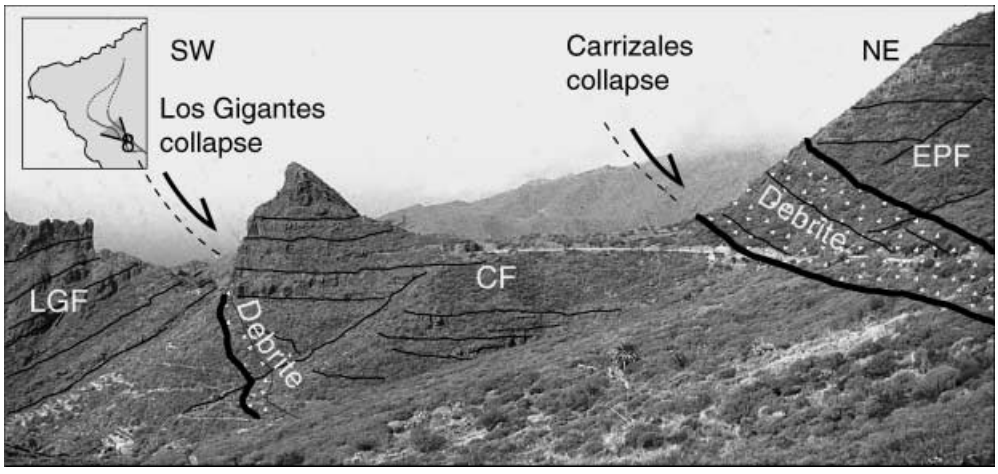

Fig. 3 Photograph of Teno unconformities. On the *left*, steeply seaward-dipping Los Gigantes Formation (*LGF*) is unconformably overlain by the subhorizontal Carrizales Formation (*CF*). About 300 m eastward, a second debrite outlines the Carrizales collapse scarp, overlain by the El Palmar Formation (*EPF*). Photo is taken from Cruz de Gilda to the northwest (*view inset*)

a horseshoe-shaped amphitheater (Fig. 2). Clasts reach decimeters in size and are mostly basaltic, the ten largest clasts in a 10-m^2 area ranging from 0.12 to 0.33 m.

The underlying Los Gigantes Formation lavas close to the unconformity are fractured. The fractures decrease in quantity and are offset with increasing distance from the unconformity. The orientation of the fractures is diffuse close to the breccia. Independent of displacement rates, the direction of the fractures is mainly scarp-parallel at a distance of 50 m west of the unconformity. East–west-directed fractures are also common, dipping 60–90°. In contrast, the dip of widespread scarp-parallel fractures is generally less inclined (50–80°), with dip lines towards and away from the unconformity. Scarp-parallel faults have minor dip-slip fault offsets (<1 m) and form synthetic and antithetic faults and small horst and graben structures.

The unconformity (scoria/lapilli and debrite deposits), as well as overlying lava flows of the Carrizales Formation, are brittle deformed by at least one younger volcano-tectonic episode that produced shear zones and slickensides (Fig. 5). Several clasts of the debrite are broken and shear zones of the overlying Carrizales lavas indicate shear sense ‘top toward the northeast’. Normal faulting was thus accomplished near this discordance after the formation of the scarp and after substantial reloading, indicating a further stage of northeast–southwest extension, with the hanging wall being located again on the northeast side.

Carrizales collapse

The scarp-replenishment lavas (Carrizales Formation) end unconformably at a second debrite (Fig. 3). The Carrizales debrite resembles the Los Gigantes debrite, being wet deposited in several episodes into a scarp. The thickness of the entire breccia unit reach about 35 m near Mazca and 20 m near Santiago del Teide. Clast sizes reach more than 1.5 m. Beside basaltic clasts, numerous clasts are rich in mafic phenocrysts (>30% Ol + Px) similar to the picritic flows of the Carrizales Formation. The diameter of the ten largest clasts on a 100-m^2 area is about 0.4 m on average. At elevations of 600–700 m (next to Mazca), the debrite dips about 35° to northeast. The unconformity is traceable for more than 7 km, encircling a second horseshoe-shaped amphitheater with an enclosed area of ~50 km^2. At deeper levels, the Carrizales debrite is largely concordant to the older one and locally has eroded into it. The horizontal distance between the bases of both unconformities varies, but reaches more than 1 km north of Carrizales. Assuming a mean parallel dip of both unconformities of 35° slightly flattening to the northeast, and a horizontal distance of 1 km, the thickness of the Carrizales Formation would originally have exceeded ~700 m.

Close to the unconformity beneath the El Palmar Formation, the Carrizales Formation lavas are strongly crashed; abundant small-scale fracture-sets disrupt the older lavas and dikes. About 50 m west of the unconformity, joint sets without obvious mismatch show average joint spacing on a 10-m transect of ~0.04 m (Fig. 6a). Younger dikes and sills are intruded erratically, and are mainly parallel to the main fracture direction surrounding the scarp. Several dikes are largely unfractured apart from cooling joints, thus younger than the second main fracture event and clearly re-used the structural zones of weaknesses. More than 200 m west of the unconformity, fracture spacing increases and the strike and dip arrangement becomes less chaotic (Fig. 6b). The number of joints decreases significantly and average joint spacing is about 0.35 m. Steeply 60–90° dipping faults show generally displacements of only some centimeters and include polished surfaces. Normal faults can rarely be traced for more than 50 m. Some normal faults show offsets of several meters, defining horst and graben structures and/or large blocks (e.g. east of Los Carrizales) of occasionally >1,000 m^3, which slumped to the north and east. The direction of extension causing this brittle deformation was northeast–southwest.

Also the debrite and magmatic replenishment of the Carrizales collapse is locally faulted by a local tectonic

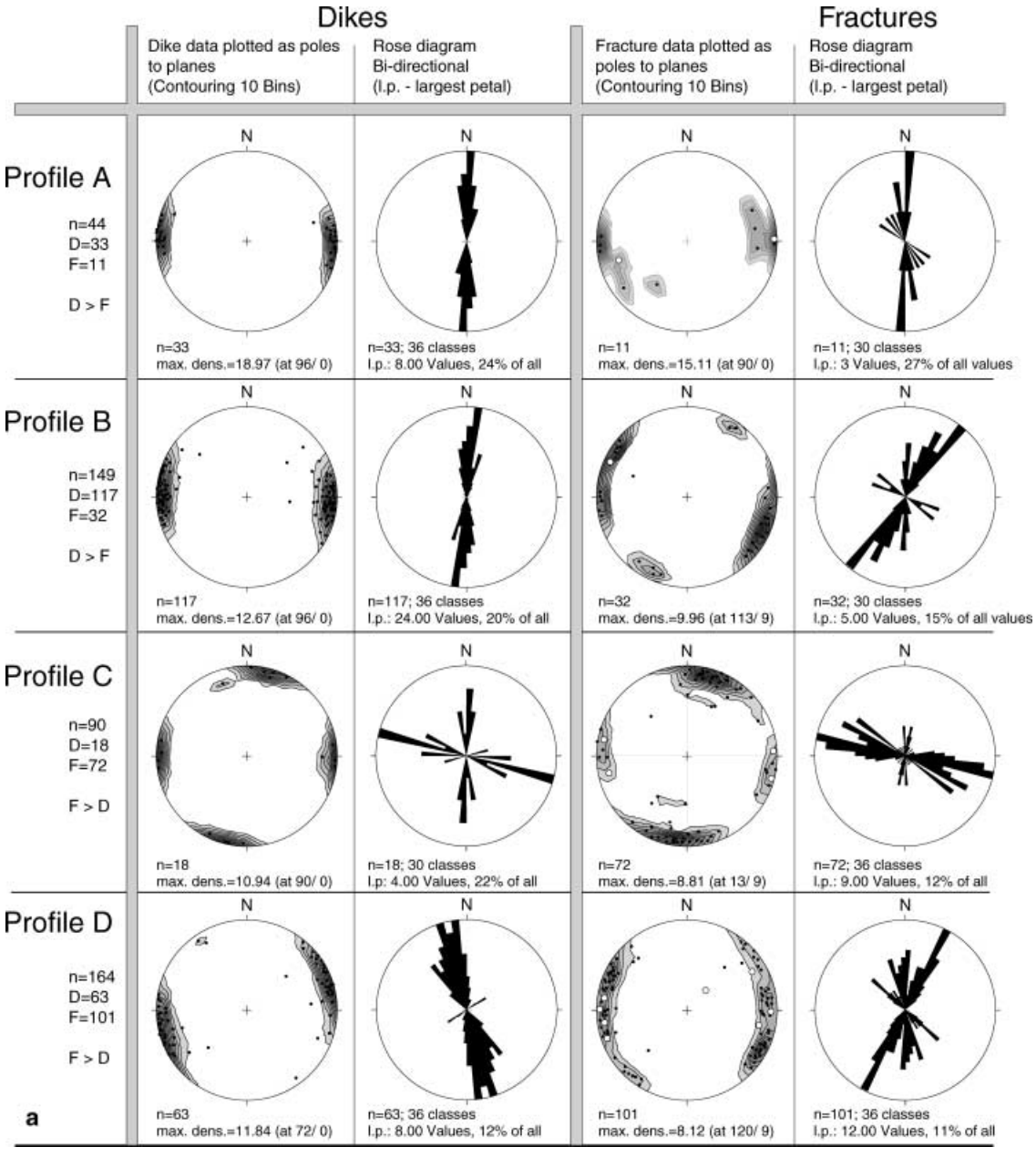

Fig. 4 Schmidt's projections, rose and contour diagrams for dikes and fractures in nine profiles through Teno massif indicated as *A–I* (see Fig. 2d). *n* Number of measurements; *D* dikes; *F* faults (*white circles*) and fractures (*black dots*)

event after subsequent infill, implying a volcano sector that was once more unstable and slightly creeping.

Teno rift zones

Teno was subjected to intense rifting before and after the northeastern sector failed. Before the edifice collapsed, at least two rift-arms converged, defining an eruptive focus centered about 2 km north–northeast of the present village of Mazca (Fig. 2b). Away from the rift zones, dikes decrease in quantity and tend to intersect and crosscut dikes of the adjacent rift zone. The rift zones define two structural axes, showing (1) a general north–south trend of dikes south of Mazca, with up to one-third of the rock volume being intrusive, and (2) a northwest–southeast trend toward Teno Bajo. A vague third southwest–northeast dike trend is largely covered and/or poorly developed (Fig. 2b, c). Both collapses of the northern sector of Teno wiped out the nucleus of the rift system, as well as large parts of the rift-axes (Fig. 2).

To estimate the dilation caused by dike emplacement (see Marinoni 2001), we measured the thickness T of a dike, the azimuth α of the computed dilation, and the strike of the dike β, giving the absolute dilation D by $D=T\sin(\alpha-\beta)$. For estimating the dilation of several

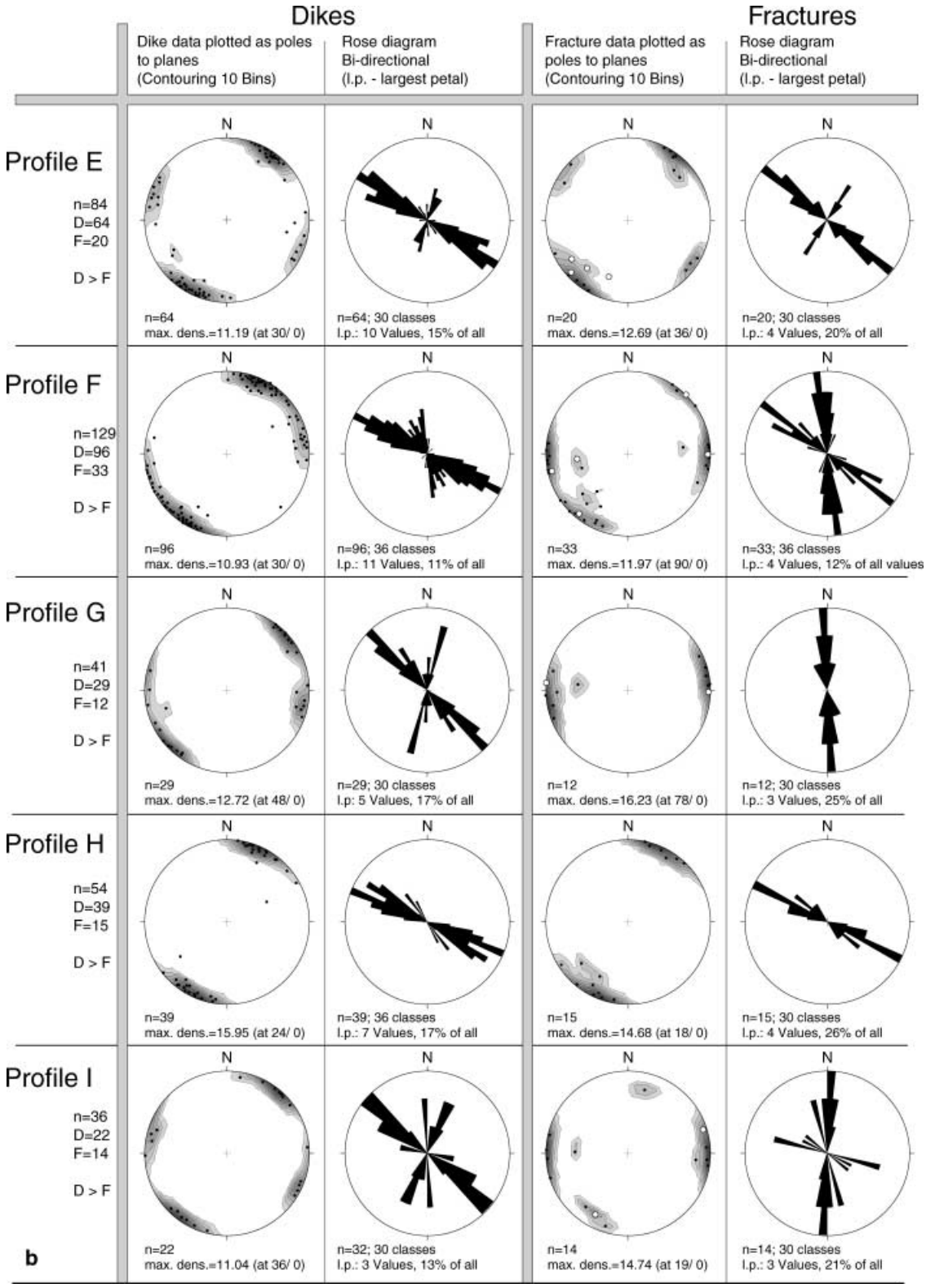

Fig. 4 Legend see page 620

dikes, the cumulative dilation was computed by the change in length (∂L) of a profile unit. This allows extensional strain computation $e=\partial L/L$, expressed as a percentage change in length. All measured orientations were corrected by the magnetic declination values, using the GEOMAG routine (US Geological Survey) based on the

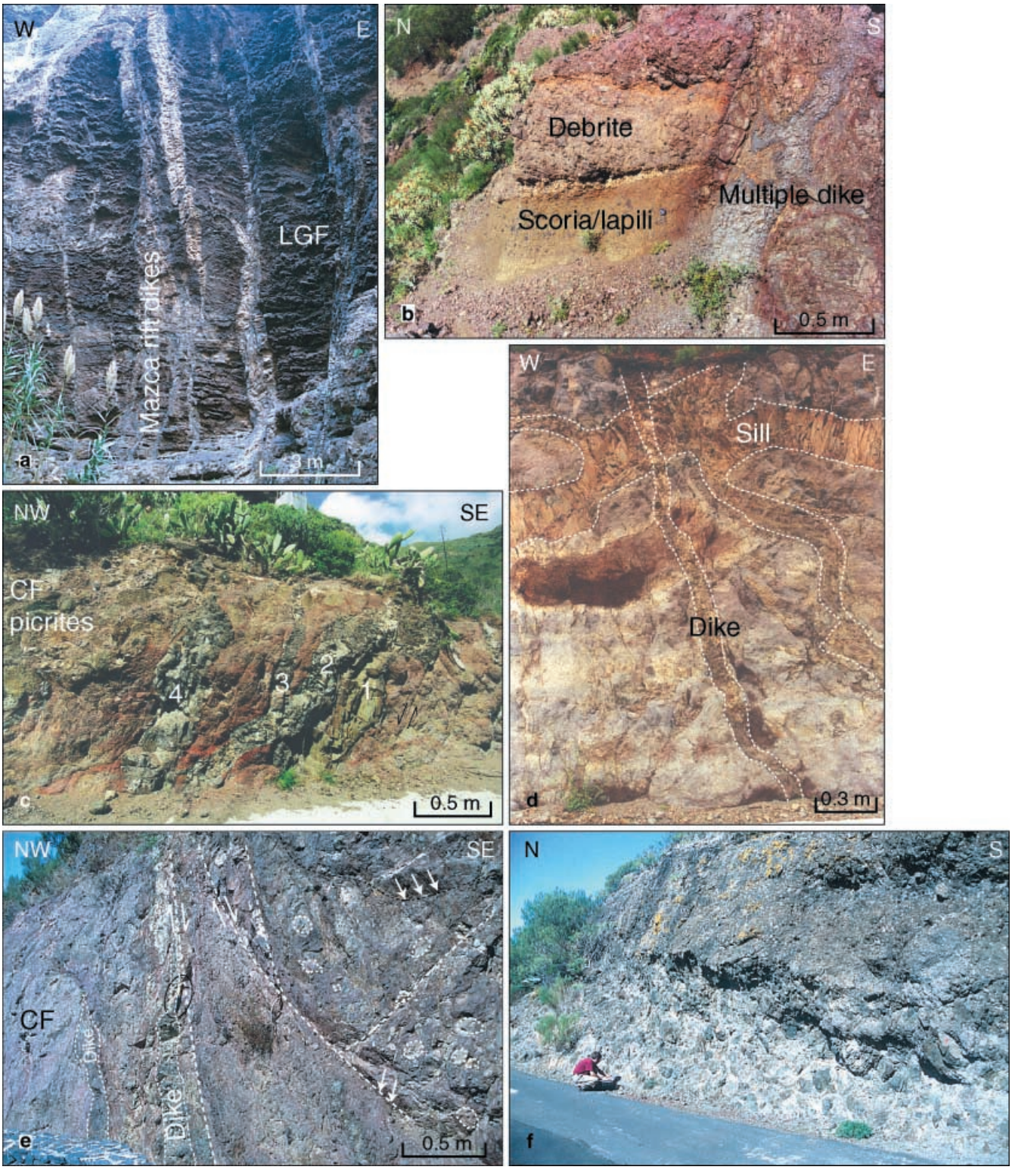

Fig. 5a Dark, very thin discontinuous pahoehoe lavas of the Los Gigantes Formation cut by light-colored dikes (Valley of Mazca, 220 m asl). **b** Debrite and scoria/lapilli deposits, defining the Los Gigantes collapse unconformity, intruded by dikes (0.5 km south of the village of Los Carrizales). **c** Picrites of the Carrizales Formation cut by four dikes of the Mazca rift zone. Locality along road profile *D*. **d** Dikes grading into columnar sills cut by younger dike in Carrizales Formation. Along road Mazca–Los Carrizales. **e** Fault zone displacing Carrizales debrites down to the NE (sector creep). Locality is east of Los Carrizales. **f** Debrites of Carrizales scarp, 30° dip to NE. Outcrop 0.5 km north of Mazca. *LGF* Los Gigantes Formation; *CF* Carrizales Formation

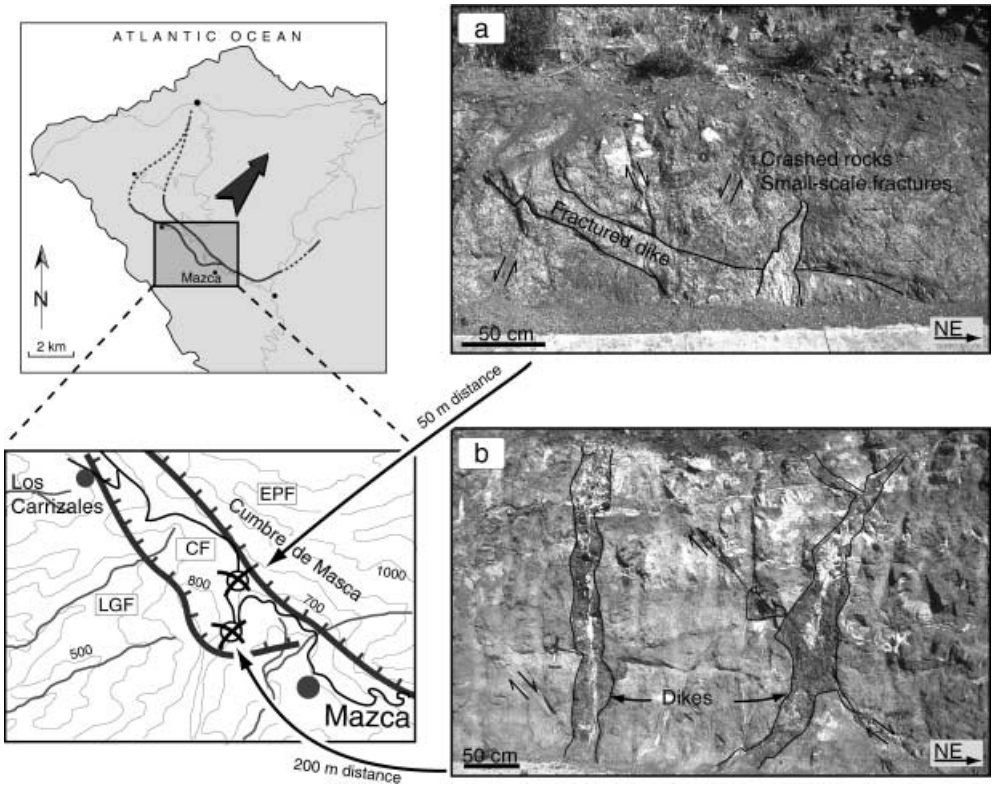

Fig. 6 Photographs of fracture belt near Los Carrizales, **a** at 50 m distance and **b** at 200 m distance from the unconformity. The fracture spacing decreases with decreasing distance to the Carrizales collapse amphitheater

current International Geomagnetic Reference Field (IGRF).

Below, we describe both main rifting trends with an attempt to separate arrangements of structures (dikes, fractures) that formed because of sector-collapse mechanisms.

The Mazca rift zone

North–south-trending dikes are mostly basaltic and frequently picritic, generally 0.6–0.8 m thick and show very constant orientations, especially in the southern sector (profile A). The dike quantity slightly increases with depth in this dike swarm and towards the inner north–south axis. In 100-m traverses, the large quantity of dikes illustrates an extensional strain of more than e=25%, computed for an area south of Mazca (Fig. 2c). Profile B shows slightly diverging orientations of dikes close to the sea, here trending more NNE–SSW. Most dikes near the shoreline of Barranco de Mazca (western profile B) are vertical (Fig. 5), but some (14 dikes) dip towards the sea with 50–70°. Significant post-intrusive fracturing is not obvious in the western part of the rift zone. Profiles B and D in total (mean dike thickness T'=0.7 m) show a horizontal east–west extension normal to the rifting axis of $\partial L_B + \partial L_D$=125 m. These profiles, however, only resemble the western part of the north–south Mazca rift. Thus, an extension exceeding 200 m is more likely for the entire Mazca rift zone.

Both landslide-related unconformities are accompanied by an immediate change in dike quantity and orientation. The dike quantity of the Mazca Rift Zone abruptly decreases from a maximum e of 28% in the Los Gigantes Formation to at most 3% within the El Palmar Formation (Fig. 2c). The intrusive activity of the Mazca Rift Zone into the intermediate Carrizales Formation is difficult to determine because this sequence is largely missing because of the younger landsliding. Following the Carrizales sector collapse, two additional trends of dikes and fractures formed concurrently to the moderately ongoing north–south dike intrusion. Near the Carrizales unconformity, one of these new trends is subparallel to the scarp (profiles C–F). Profile C comprises 90 measurements of dikes (18) and fractures (72), showing trends from N015° to N110° (Fig. 4). In profile C, the Mazca rift axis no longer prevails in the El Palmar Formation. The bulk intrusive activity of the Mazca Rift Zone was thus earlier than the Carrizales collapse.

The number of fractures increases significantly toward this unconformity in profiles C–F. The mean fracture directions are N110° (profile C), N30° and N175° (profile D), N130° (profile E) and N170° (profile F). Profile D west of the unconformity along the road cut between Mazca and Degollada de Cherfe also shows a general north–south (N170°) dike arrangement of the Mazca Rift Zone. In total, a local bimodal arrangement is shown by the structural data near the unconformities (profiles C–D, Fig. 4), moreover, thin sills (<30 cm) are common along profile D (Fig. 5). Because of the systematic variance of fractures near an unconformity, the brit-

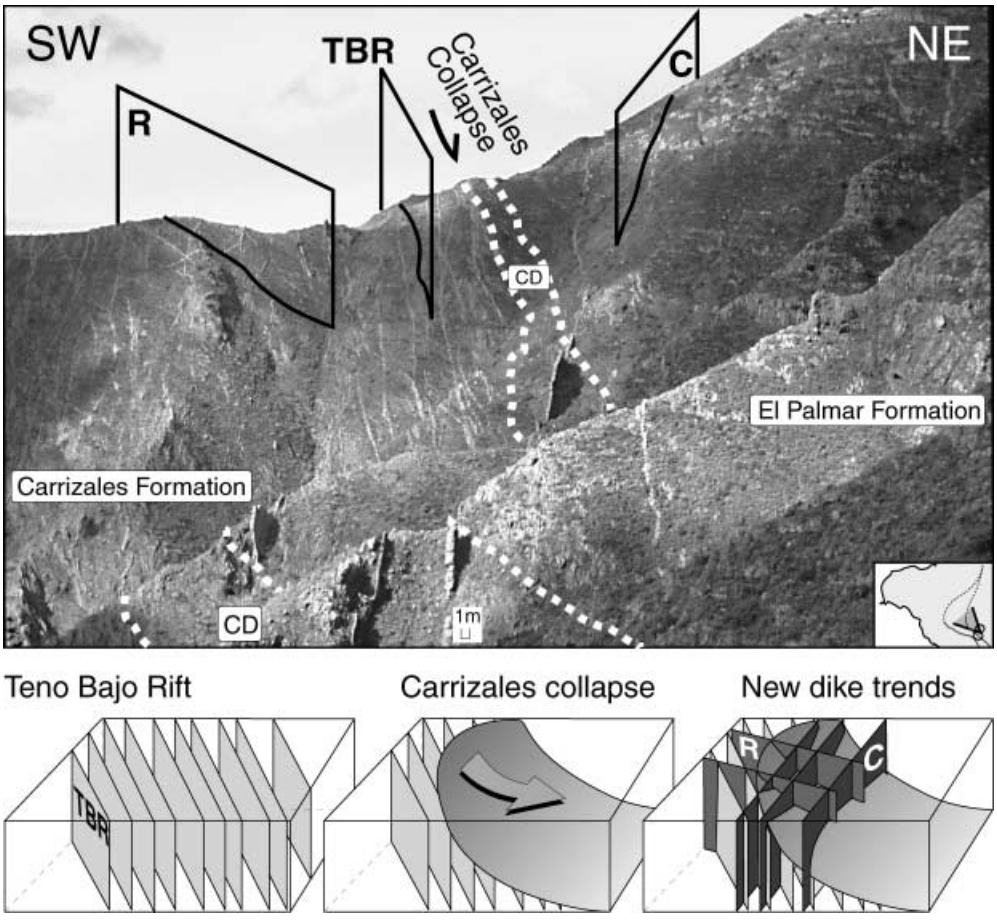

Fig. 7 Photograph taken from La Tabaiba to the northwest (*view insert*), showing Carrizales and El Palmar Formation, separated by Carrizales debrites (*CD*). Dike swarm of the Teno Bajo Rift (*TBR*) is clearly cut-off at the unconformity. Younger dikes intruded concentrically (*C*) and, to a lesser degree, radially (*R*) into the El Palmar and Carrizales Formation. The debrite of the older Los Gigantes collapse crops out ~1 km west of CD

tle deformation is likely related to sector failure rather than to rifting. Marinoni and Gudmundsson (2000) analyzed the same road cut (our profile D) and also found a general northeast–southwest extension. Moreover, dikes younger than the majority of Mazca Rift dikes have orientations very much resembling those of the fractures (Fig. 4). The post-Carrizales collapse maximum horizontal extensional strain measured by concentric dikes was only 5% near Mazca.

The north–south dikes maintain their vertical dip away from the main intrusive axis of the Mazca rift zone, but decrease in quantity and crosscut, and are crosscut by dikes of the accompanying northwest–southeast rift. In the Los Gigantes Formation, profile E summarizes the data in the distal part of two main rift zones of Teno, with intersecting trends of the (here minor developed) Mazca rift and the northwest–southeast-directed dikes.

Teno Bajo rift zone

This northwest–southeast trend dissects the succession by hundreds of dikes, presumably jointly responsible for the northwest elongated morphological shape of Teno. The basaltic dikes are generally thinner than 1 m, whereas more evolved trachyandesitic to phonolitic dikes (mostly outcropping near the northern shoreline) reach more than 6 m, with multiple dikes more than 12 m in width. The dike direction did not change significantly following the Los Gigantes collapse. However, broad outcrops of the Teno Bajo Rift Zone are limited to northwestern Teno Alto and to the area north of the village Los Carrizales. They have since became covered or obscured by younger volcanic episodes. Both unconformities result in a sudden discontinuity of the northwest–southeast dike quantity. Intrusion continued, with pronounced dike emplacement in the Carrizales Formation (Fig. 7).

Following the Carrizales collapse and the El Palmar Formation, intruding dikes crosscut the pre-collapse dikes of the Teno Bajo Rift Zone at an acute angle. These reconfigured dikes may imply that the structural axis of the rift rotated slightly (10–30°) after sector collapse(s) (Fig. 7). Profile F summarizes trends of dikes oriented generally N125°. From the sum of 96 dikes, 71 dikes with an average T=0.8 m show a northeast–southwest extension of about ∂L=57 m. An extensional strain for 21 scarp-circumscribing dikes that intruded the Carrizales Formation of ∂L=25 m in direction ENE–WSW is computed. The El Palmar Formation is intruded by only a small number of northwest–southeast dikes of the Teno Bajo Rift Zone (profile F). Hence, the activity of the Teno Bajo Rift decreased in this region,

whereas the amount of concentric dike trends increases (Fig. 7). Concentric dikes are slightly curved and/or arranged in an en–echelon fashion close to the weakened unconformity. Towards the northern shoreline of Teno, the quantity of dikes that circumscribes the scarp of the sector-collapses decreases (compare with profile G), whereas the N130° Teno Bajo Rift trend prevails (profile H). Moreover, dikes in the large valley of El Palmar are also generally oriented comparable to the Teno Bajo Rift Zone, suggesting an extension directed northeast–southwest, there still existing after the bulk of the El Palmar Formation had been emplaced.

The fracture belt(s)

The spacing of fractures along individual profiles is generally inhomogeneous. Most profiles located radially away from landslide unconformities show a decrease in fracture quantity. A characteristic 100-m traverse unit of profile A did not reveal significant fracturing. In contrast, a 100-m unit of profile C, D or eastern profile B exposes displacing fracture quantities that range on average from 20 (B) to 50 (C) fractures. Profile-parallel fractures may have been underestimated, however.

Because fracturing within the rift zones is negligible at a distance from the scarps, rifting as a main cause for fracturing seems unlikely (profiles A and H). Moreover, fracturing increases with decreasing distance from the unconformities and thus reflects the large structural influence of the unstable northern flank of Teno. In close-up, the fracture quantity increases from west towards the first unconformity (Los Gigantes collapse), then slightly decreases, and strongly increases again towards the second unconformity formed by the Carrizales collapse. In the El Palmar Formation, fracture spacing is large again. Sorting out the trends of the rift zones, the orientation of the fractures of profiles B–G show two main trends: concentric and diffuse-radial relative to the unconformity(ies). This fracture belt with bimodal orientations resembles those non-rift-trends of dikes near the unconformities.

Discussion

Volcano sector collapse associated with rift zone-bounded flanks is one of the most common destructive events during the evolution of volcanic oceanic islands (Siebert 1984). Giant landslides in the Canary Islands are thought to be triggered by accumulative tensional stresses, which include long-lasting stresses resulting from progressive edifice growth/construction, cumulative stresses by dike intrusions plus ephemeral stresses such as local seismicity (Carracedo 1994).

In Teno, a Miocene composite shield volcano in northwestern Tenerife, three successive formations are separated by landslide unconformities, indicating episodically alternating constructive and destructive evolutionary stages. The rapidity of these constructive and destructive events is remarkable, including at least two giant landslides and subsequent huge scar replenishments, all probably within less than 0.5 Ma (age data of Thirlwall et al. 2000; Bogaard, unpublished data). The northern and southern regions of Teno were under different extensional stress fields, being east–west in southern and northeast–southwest in central and northern Teno. There is no evidence for regional tectonic influences to have affected the entire Teno shield. The tensional stresses are constrained by two main rift zones (north–south and northwest–southeast); a (minor) third northeast–southwest rift zone may have been active as a local tension consequence of the compression induced by dilation of the two main rift zones. Dike emplacement rates along the rift zones decreased with time, showing the main tensional stress to have acted prior the recurrent lateral collapse.

The establishment and orientation of a fractured belt flanking the sector collapse-related palaeo-scarps on Teno shows no structural relationship with preceding rift zone positions and dike directions. Such fracture zones may be the combined result of localized fault zones with a set of associated shear fractures formed by a progressive creeping sector, followed by rapid decompression of initially underlying parts during sector collapse. Along the profiles, the quantity of faults and fractures as opposed to the quantity of dikes varies strongly and thus allows a definition of the site of maximum brittle deformation (profiles C, D) to have been located between the villages of Mazca and Los Carrizales. Here, moreover, numerous thin sills were intruded into the Carrizales Formation beneath the unconformity (Fig. 5). Some sills are strongly fractured, others not, indicating intrusive activity prior and subsequent to the Carrizales collapse, possibly further weakening or lubricating the décollement.

The Carrizales Formation lavas, in particular, are increasingly fractured with decreasing distance to the second unconformity. The concentric and subordinate radial structural systems delineating the scarp are in part similar to configurations known from structural doming. In the landslide case of Teno, however, the concentric trend clearly prevails. Such a horseshoe-shaped structural pattern of dikes and fractures provides a clue to the hidden unstable flank and/or palaeo-scarp location. In northern Teno, the Los Gigantes and Carrizales sector collapse scarps are largely covered or eroded by smaller landslides and, thus, are difficult to define. However, some of the dike and fracture trends are apparently semi-concentric, suggesting the continuation of the buried unconformities to be located nearby (Figs. 2 and 4). Based on the structural pattern around the rim of ancient headwalls in Teno, we suggest that if dikes and fractures on volcano flanks do not fit the general tectonic and/or rift zone pattern, the nearby site of an ancient sector collapse or creeping flank should be considered.

Fiske and Jackson (1972) showed that the orientation and evolution of a dike swarm depends upon near-surface stress fields; hence stress field changes because of

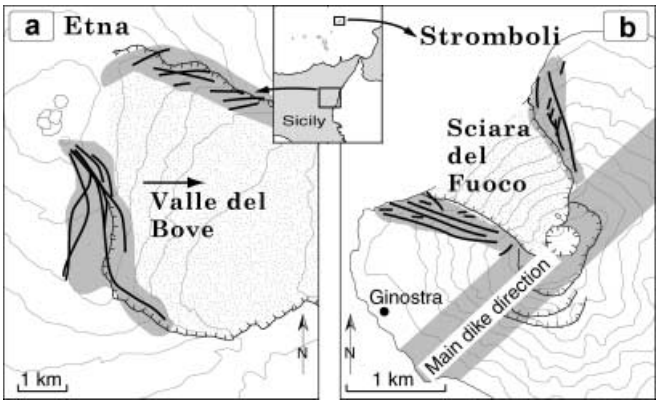

Fig. 8a Map showing the traces of dikes emplaced on the upper southeastern flank of Etna between 1978 and 1991 as inferred from deformation measurements. Modified after Ferrari et al. (1991) and McGuire et al. (1997). **b** The Sciara del Fuoco depression is related to multiple sector collapses (after Tibaldi 2001). Dike swarms of Neostromboli material on both sides of the Sciara indicate that zones of weakness already developed during that period, probably heralding the collapse

volcano flank instability may adjust their orientation. This relationship has been demonstrated for the lateral failure of Valle del Bove on Etna (McGuire et al. 1990) and Sciara del Fuoco on Stromboli (Tibaldi 2001), illustrating dike re-orientation, with the overall elongation of the swarm approximately following the rim of the headwall (Fig. 8). In Teno, new dike directions were established close to the unconformities, indicating a local change of the palaeo-stress field at the time of dike emplacement. Recurrent sector collapse events at Stromboli Volcano took place whenever the scarp-replenishing sequence reached an almost similar height and volume (Tibaldi 2001). In Teno, the outline of the first collapse largely encircles the younger scarp in plan view; thus the first collapse was the largest, a structural relationship similar to that on Stromboli (Tibaldi 2001). When the accumulating mass of scarp-replenishments reaches a critical threshold, the edifice could collapse solely under its own load (cf. Voight and Elsworth 1997). Presumably, the intensely fractured zone surrounding the palaeo-scarp in Teno underlies the former décollement also at depth, and mechanically influenced the edifice stability when reloaded by younger formations. A similar zone of weakness could have been involved in recurrent sector failures of Stromboli. The semi-concentric dike orientations in Teno reflect an extensional stress close to the scarps, which is most pronounced after infill/replenishment of the depression (Fig. 9). The semi-concentric dike orientation indicates lateral creeping of the replenishing sequence. The most vulnerable surface for this detachment is assumed to be the destabilized and fractured neighborhood of the earlier sector collapse footwall. Moreover, the influence of the weak zone in Teno may have become amplified by alteration, resulting in a reduction in confined and unconfined rock strength, cohesion, friction and unit weight (Hürlimann et al. 1999; Watters et al. 2000). The concentric direction of younger dikes, thus, may well be a response of recurrent sector creep and – once established – increases the stress acting

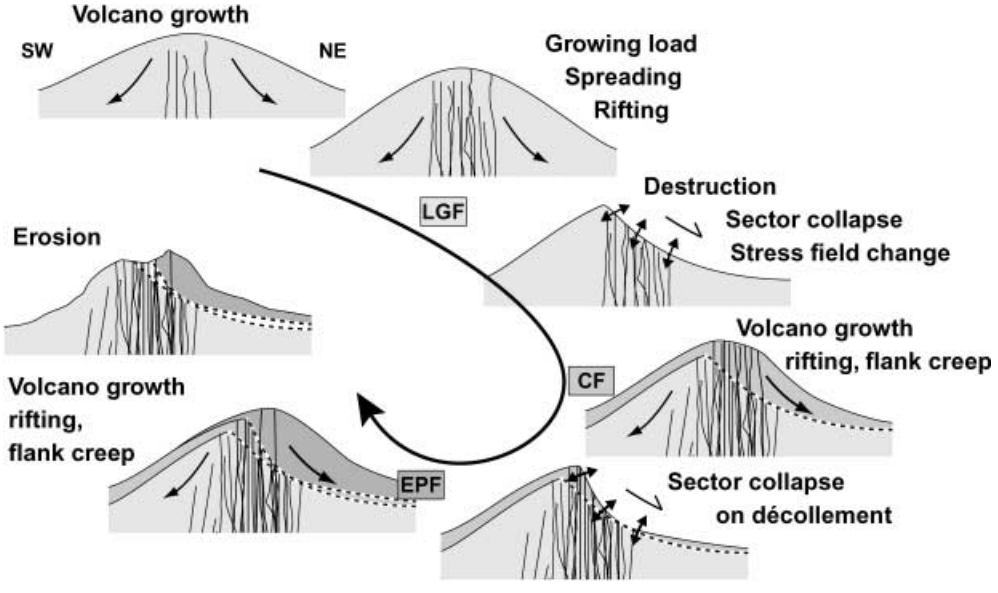

Fig. 9 Cycle of volcano construction and destruction. The growing load of the volcano causes gravitational spreading, expansion and focuses rifting. When the stability threshold is exceeded, the flank fails and collapses into the sea. This mass wasting is often accompanied by a change in stress field orientation, decompression of the magmatic system and rapid scarp infill. Subsequent scarp-replenishment emplaced on top of the earlier debrites and the structurally weakened footwall. The increasing load gradually enhances flank creep and dike reorientation. The stability is again surpassed and recurrent sector collapse occurs, recycling the former décollement vicinity. This cycle may be repeated several times, or stops if magmatic activity and loading decline. *LGF* Los Gigantes Formation; *CF* Carrizales Formation; *EPF* El Palmar Formation

on the encircled flank. Probably the infilled scarp slightly sagged due to its load, producing a lateral creep in the former scarp region – there resulting in extension that might be interpreted as structures that form by an aborted landslide.

The Carrizales collapse scarp was replenished by lavas of the El Palmar Formation that reached a thickness of >700 m. Although this replenishment was voluminous, it did not fail in a third giant NNW-directed flank collapse. Our dike data imply that the highest intrusion rates occurred prior to the Carrizales collapse. The northwestern flank of the El Palmar Formation was initially creeping, and then intrusive activity parallel the scarp largely stopped. Conceivably, the load was not sufficiently high to cause failure, whereas intrusions and accompanied pressure variances could no more lubricate the weak zone beneath. The subaerial structure of the Teno edifice was henceforth principally stable, the stability being enhanced by a decrease in eruption rates.

Conclusion

Geometrically similar giant landslides took place in the northern part of the Miocene Teno shield volcano complex on Tenerife, defining three unconformity-bounded formations (LGF, CF, EPF). Two main rift zones indicate generally contemporaneous extensions that are northeast–southwest in northern and east–west in southern Teno, and most of those dikes were emplaced prior to the Carrizales flank failure.

Recurrent landslide mass transfer caused intense fracturing in the normal fault footwall, shown in Teno as a girdle of fractures that delineates the landslide scarp. Subsequently, younger lavas of the replenishment phase were largely positioned on the structurally weak plane. A volcano sector situated on such a potential décollement is most susceptible to become the site of future flank collapses or flank creep. Recurrent episodes of volcano construction and destruction are escorted by a change of the direction of dikes in Teno, reorganizing from narrow rift zones to semi-concentric dike arrangements encircling the palaeo-scarps. The recurrent volcano landslides largely changed the structural configuration and thus the subsequent evolution of the volcano.

Acknowledgements We thank Pepe Navarro for discussions and introducing us to the geological magnificence of Tenerife. Thanks to A. Belousov for comments and suggestions in field. This paper benefited from very constructive reviews of L. Marinoni, A. Gudmundsson and C. Stillman. The paper is part of the PhD thesis of T.R.W. This project was supported by the Deutsche Forschungsgemeinschaft (DFG grant Schm 250/77-1), the graduate school 'Dynamics of Global Cycles' (DFG grant Schm 250-49) and the Land Schleswig-Holstein.

References

Ablay GJ, Hürlimann M (2000) Evolution of the north flank of Tenerife by recurrent giant landslide processes. J Volcanol Geotherm Res 103:135–159

Ancochea E, Fúster JM, Ibarrola E, Cendrero A, Coello J, Hernan F, Cantagrel JM, Jamond C (1990) Volcanic evolution of the island of Tenerife (Canary Islands) in the light of new K–Ar data. J Volcanol Geotherm Res 44:231–249

Anderson EM (1937) Cone sheets and ring dykes; the dynamical explanation. Bull Volcanol 1:35–40

Barrera JL, Gomez JA, Bellido F (1989) Mapa geológico de España, E. 1:25,000. IGME, Madrid

Borgia A (1994) Dynamic basis of volcanic spreading. J Geophys Res 99:17791–17804

Cantagrel JM, Arnaud NO, Ancochea E, Fúster JM, Huertas MJ (1999) Repeated debris avalanches on Tenerife and genesis of Las Cañadas caldera wall (Canary Islands). Geology 27:739–742

Carracedo JC (1994) The Canary Islands: an example of structural control on the growth of large oceanic-island volcanoes. J Volcanol Geotherm Res 60:225–241

Carracedo JC (1996) Morphological and structural evolution of the western Canary Islands: hotspot induced three-armed rifts or regional tectonic trends? J Volcanol Geotherm Res 72:151–162

Day SJ, Carracedo JC, Guillou H, Gravestock P (1999) Recent structural evolution of the Cumbre Vieja volcano, La Palma, Canary Islands: volcanic rift zone reconfiguration as a precursor to volcano flank instability? J Volcanol Geotherm Res 94:135–167

Féraud G, Giannerini G, Campredon R, Stillman CJ (1985) Geochronology of some Canarian dyke swarms. Contribution to the volcano-tectonic evolution of the archipelago. J Volcanol Geotherm Res 25:29–52

Ferrari L, Garduño V-H, Neri M (1991) I dicchi della Valle del Bove, Etna: un metodo per stimare le dilatazioni di un apparato vulcanico. Mem Soc Geol It 47:495–508

Fiske RS, Jackson ED (1972) Orientation and growth of Hawaiian volcanic rifts: the effect of regional structure and gravitational stress. Proc R Soc Lond 329:299–320

Hürlimann M, Ledema A, Martí J (1999) Conditions favouring catastrophic landslides on Tenerife (Canary Islands). Terra Nova 11:106–111

Krastel S, Schmincke H-U, Jacobs CL, Rihm R, La Bas TP, Alibés B (2001) Submarine landslides around the Canary Islands. J Geophys Res 106:3977–3997

Marinoni LB (2001) Crustal extension from exposed sheet intrusions: review and method proposal. J Volcanol Geotherm Res 107:27–46

Marinoni LB, Gudmundsson A (2000) Dykes, faults and palaeostresses in the Teno and Anaga massifs of Tenerife (Canary Islands). J Volcanol Geotherm Res 103:83–103

Martí J, Ablay GJ, Bryan S (1996) Comment on the Canary Islands: an example of structural control on the growth of large oceanic-islands volcanoes by JC Carracedo. J Volcanol Geotherm Res 72:143-149

Martí J, Hürlimann M, Ablay GJ, Gudmundsson A (1997) Vertical and lateral collapses on Tenerife (Canary Islands) and other volcanic ocean islands. Geology 25:879–882

McFarlane DJ, Ridley WI (1968) An interpretation of gravity data for Tenerife, Canary Islands. Earth Planet Sci Lett 4:481–486

McGuire WJ, Pullen AD, Saunders SJ (1990) Recent dyke-induced large-scale block movement at Mount Etna and potential slope failure. Nature 343:357–359

McGuire WJ, Stewart IS, Saunders SJ (1997) Intra-volcanic rifting at Mount Etna in the context of regional tectonics. Acta Volcanol 9:147–156

Navarro JM, Coello J (1989) Depressions originated by landslide processes in Tenerife. European Science Foundation Meeting on Canarian Volcanism, pp 149–152

Navarro JM, Farrujia I (1989) Plan Hidrológico Insular de Tenerife. Zonificación hidrogeológía, aspectos geológicos e hidrogeológicos. Cabildo Insular de Tenerife

Schmincke H-U (1968) Faulting versus erosion and the reconstruction of the mid-Miocene shield volcano of Gran Canaria. Geol Mitt 8:23–50

Schmincke H-U, Navarro JM, Sumita M (1999) A giant blast associated with flank collapse of the Cañadas Volcano (Tenerife, Canary Islands) 0.18 M.y. ago. EUG 10, Terra Nostra J Conf Abstr 4:753

Siebert L (1984) Large volcanic debris avalanches: characteristics of source areas, deposits and associated eruptions. J Volcanol Geotherm Res 22:163–197

Stillman CJ (1987) A Canary Islands dyke swarm: implications for the formation of oceanic islands by extensional fissural volcanism. In: Halls HC, Fahrig WJ (eds) Mafic dyke swarms. Geol Assoc Can Spec Pap 34:243–255

Teide Group (1997) Morphometric interpretation of the northwest and southeast slopes of Tenerife, Canary Islands. J Geophys Res 102:487–498

Thirlwall MF, Singer BS, Marriner GF (2000) 39Ar–40Ar ages and geochemistry of the basaltic shield stage of Tenerife, Canary Islands, Spain. J Volcanol Geotherm Res 103:247–297

Tibaldi A (2001) Multiple sector collapses at Stromboli Volcano, Italy: how they work. Bull Volcanol 63:112–125

Voight B, Elsworth D (1997) Failure of volcano slopes. Geotechnique 47:1–31

Walker GPL (1992) Coherent intrusion complexes in large basaltic volcanoes – a new structural model. J Volcanol Geotherm Res 50:41–54.

Watters RJ, Zimbelman DR, Bowman SD, Crowley JK (2000) Rock mass strength assessment and significance to edifice stability, Mount Rainier and Mount Hood, Cascade Range volcanoes. Pure Appl Geophys 157:957–976

Watts AB, Masson DG (2001) New sonar evidence for recent catastrophic collapses of the north flank of Tenerife, Canary Islands. Bull Volcanol 63:8–19